Contrast masking in strabismic amblyopia: attenuation, noise, interocular suppression and binocular summation

Daniel H. Baker[a,b], Tim S. Meese[a], Robert F. Hess[b]

[a]School of Life and Health Sciences, Aston University, Birmingham, B4 7ET, UK
[b]McGill Vision Research Unit, Dept. Ophthalmology, McGill University, Montreal, Quebec, Canada
email: d.h.baker1@aston.ac.uk

Abstract

To investigate amblyopic contrast vision at threshold and above we performed pedestal masking (contrast discrimination) experiments with a group of eight strabismic amblyopes using horizontal sinusoidal gratings (mainly 3 c/deg) in monocular, binocular and dichoptic configurations balanced across eye (i.e. five conditions). With some exceptions in some observers, the four main results were as follows. 1) For the monocular and dichoptic conditions, sensitivity was less in the amblyopic eye than in the good eye at all mask contrasts. 2) Binocular and monocular dipper functions superimposed in the good eye. 3) Monocular masking functions had a normal dipper shape in the good eye, but facilitation was diminished in the amblyopic eye. 4) A less consistent result was normal facilitation in dichoptic masking when testing the good eye, but a loss of this when testing the amblyopic eye. This pattern of amblyopic results was replicated in a normal observer by placing a neutral density filter in front of one eye. The two-stage model of binocular contrast gain control (Meese, Georgeson and Baker, 2006; JoV, 6: 1224-1243) was 'lesioned' in several ways to assess the form of the amblyopic deficit. The most successful model involves attenuation of signal and an increase in noise in the amblyopic eye, and intact stages of interocular suppression and binocular summation. This implies a behavioural influence from monocular noise in the amblyopic visual system as well as in normal observers with an ND filter over one eye.

Keywords: human vision, amblyopia, strabismus, masking, contrast discrimination, noise

1 Introduction

1.1 Pedestal masking in normal observers

A successful approach to understanding normal contrast vision (Rohaly, Ahumada & Watson, 1997; Clatworthy, Chirimuuta, Lauritzen & Tolhurst, 2003; Parraga, Troscianko & Tolhurst, 2005; Zhang, Pham & Eckstein, 2006; Bex, Dakin & Mareschal, 2007) has been to measure contrast increment thresholds (contrast discrimination) for a wide range of pedestal (background) contrasts (Campbell & Kulikowski, 1966; Nachmias & Sansbury, 1974; Legge, 1979; Legge & Foley, 1980; Burton, 1981; Foley, 1994; Meese, 2004; Meese *et al.*, 2006; Meese & Summers, 2007). These studies indicate how the signal to noise ratio varies across the visual system's dynamic range for luminance contrast. When pedestal and test gratings are monocular (i.e. both presented to the same eye), contrast discrimination functions are dipper-shaped, with a region of facilitation at low pedestal contrasts and a region of masking with a log-log slope of around 0.6 at higher pedestal contrasts (Campbell & Kulikowski, 1966; Nachmias and Sansbury, 1974; Legge & Foley, 1980). Binocular dipper-functions are very similar to the monocular variety, but detection threshold (pedestal contrast = 0%) and the region of facilitation are offset downwards owing to the binocular advantage (Legge, 1984; Meese *et al*, 2006). Dichoptic

presentation (where pedestal[1] and test gratings are presented to different eyes) produces weaker facilitation (Blake and Levinson, 1977; Levi *et al.*, 1980; Meese *et al.*, 2006) and stronger masking (Legge, 1979; Maehara & Goryo, 2005; Meese *et al.*, 2006) than the other two varieties. These differences mean that there must be a nonlinearity before the binocular combination of lumiance contrast across the eyes. Interocular suppression (Baker & Meese, 2007) and nonlinear contrast transduction (Meese, Georgeson & Baker, 2007) are both viable candidates.

1.2 Pedestal masking in amblyopic observers

Although there have been numerous studies of suprathreshold spatial deficits in amblyopia (e.g. Hess & Field, 1994; Popple & Levi, 2000; Hess, Dakin, Tewfik & Bown, 2001; Barnes et al, 2001; Hess, Pointer, Simmers & Bex, 2003; McKee, Levi & Movshon, 2003; Levi, Li & Klein, 2005; Simmers, Ledgeway & Hess, 2005; Li, Dumoulin, Mansouri & Hess, 2007; Levi, Klein & Chen, 2007; Levi, 2007; Levi, Yu, Kuai & Rislove, 2007) there has not been a detailed study of pedestal-masking for gratings in which the three ocular arrangements (monocular, binocular and dichoptic) have been measured (see section 5.1. for review). This is unfortunate because it was only by considering these functions together that sufficient constraints were found to shed light on the organization of normal contrast vision (see section 1.4). And as amblyopic defecits might arise from amplifications of otherwise normal visual operations (Harrad & Hess, 1992), it is important to perform these experiments on amblyopes to more fully characterize their contrast vision.

1.3 Amblyopic effects at contrast detection threshold

Although there have been few contrast-increment studies above threshold, much more is known about amblyopic spatial vision at detection threshold. One of the best known deficits is the loss of contrast sensitivity in the amblyopic eye (Hess & Howell, 1977; Levi & Harwerth, 1977; Bradley and Freeman, 1981; Asper *et al.*, 2000), thought by some to be the long-term consequence

of amblyopic suppression (Sengpiel & Blakemore, 1996). Psychophysical testing has suggested that several factors might be involved, including fewer active cells (Levi *et al.*, 1987), inhibition between the eyes (Sengpiel & Blakemore, 1996; Pardhan & Gilchrist, 1992) high levels of noise (Huang *et al.*, 2007; Levi & Klein, 2003; Levi, Klein & Chen, 2007, 2008), and disorganisation of visual neurons (Hess and Field, 1994).

Another widespread finding at detection threshold is that there is little or no benefit in using two eyes instead of one (Lema and Blake, 1977; Levi *et al.*, 1979, 1980; Pardhan and Gilchrist, 1992; Hood and Morrison, 2002; Holopigian *et al.*, 1986). This might be because the neural mechanisms of summation are compromised, perhaps owing to the loss of binocular connections. However, for horizontal gratings we have found that binocular summation is normal in strabismic amblyopes when the contrast is normalized to the sensitivity of each eye (Baker, Meese, Mansouri and Hess, 2007b). This indicates that at least some binocular summation mechanisms are intact, and that the absence of empirical summation using conventional testing (Lema and Blake, 1977; Levi *et al.*, 1979, 1980; Holopigian *et al.*, 1986; Pardhan and Gilchrist, 1992; Hood and Morrison, 2002; McKee, Levi & Movshon, 2003) might be attributable to the different sensitivities between the eyes.

1.4 A computational approach to binocular interactions

Detailed computational models of the amblyopic deficits in contrast vision have not been developed, partly because there has been little consensus over the form of binocular interactions in the normal early visual system (Campbell & Green, 1965; Legge & Rubin, 1981; Legge, 1984; Legge & Gu, 1989; Kontsevich & Tyler, 1994; Stevenson & Cormack, 2000; Ding & Sperling, 2006). In a recent series of experiments we have redressed the issue of binocular interactions in normal observers using parallel (Meese, Georgeson & Baker, 2006; Baker, Meese & Georgeson, 2007a; Baker & Meese, 2007) and cross-oriented gratings (Baker, Meese & Summers, 2007c) presented to the same or different eyes. From these studies we developed the two-stage model of contrast gain control (Meese et al, 2006) where the first stage is placed before the binocular summation of signals but receives suppressive input from the other eye (Baker et al 2007c; Baker & Meese, 2007). This model provides a good account of a wide variety of phenomena (see Baker & Meese, 2007 for a brief

---

[1] The terms 'pedestal' and 'mask' are not used consistently in the literature. In this paper we use the term pedestal to mean a mask that has the same spatial frequency, orientation, phase, size and stimulus duration as the target. According to this definition, the term 'pedestal' is applicable to all of the experimental conditions that we investigated. We also use 'pedestal masking', 'masking function' and other similar phrases to refer to the results from our experiments.

review), including contrast summation, detection and discrimination (Meese et al, 2006) and contrast-matching (Baker, Meese & Georgeson, 2007a).

1.5 Overview

Here, we extend our understanding of amblyopic contrast vision by measuring contrast-masking functions in a group of strabismic amblyopes for monocular, binocular and dichoptic presentations of horizontal gratings (see Baker, Meese, Mansouri & Hess, 2007b for detailed analysis of the detection thresholds). Our aim was to identify candidate causes of visual dysfunction by determining how the two-stage model of contrast gain control (Meese et al, 2006) could be disturbed to simulate the abnormalities in the amblyopic data. In addition, the experiments were performed by a normal control observer both with and without a neutral density (ND) filter in front of one eye. Although the ND filter scales the luminance of the entire stimulus in the relevant eye it does not change its contrast. Nevertheless, contrast sensitivity declines with a decrease in mean lumince (Van Nes & Bouman, 1967; DeValois, Morgan & Snodderly, 1974) and so peformance in the filtered eye should be compromised. Indeed, this manipulation has been shown to produce 'amblyopic' behaviour in normals in several experimental paradigms (Gilchrist and McIver, 1985; Heravian-Shandiz *et al.*, 1991; de Belsunce and Sireteanu, 1991; Leonards and Sireteanu, 1993; Baker *et al.*, 2007b) as well as 'normal' behaviour in amblyopia (Hess, Campbell and Zimmern, 1980), and we wondered whether this comparison would extend to the conditions here.

2 Methods

2.1 Apparatus and Stimuli

Stimuli were patches of horizontal sinusoidal grating, spatially modulated by a raised cosine envelope with a central plateau of 3° and a cosine half-period of 1°. Their spatial frequency was 3 c/deg (15 full cycles per patch before applying the window; see Fig 1A). For one observer (EGF), detection thresholds at 3 c/deg were unmeasurable in the amblyopic eye. For this observer, 0.5 c/deg gratings were used, with the same spatial envelope as above (see Fig 1A). The normal control subject, DHB, also completed the experiment at 0.5 c/deg. All stimuli were displayed on a Clinton Monoray monitor with a framerate of 120Hz (mean luminance 200cd/m²), using a VSG 2/5 (Cambridge Research Systems Ltd., Kent, UK) controlled by a PC.
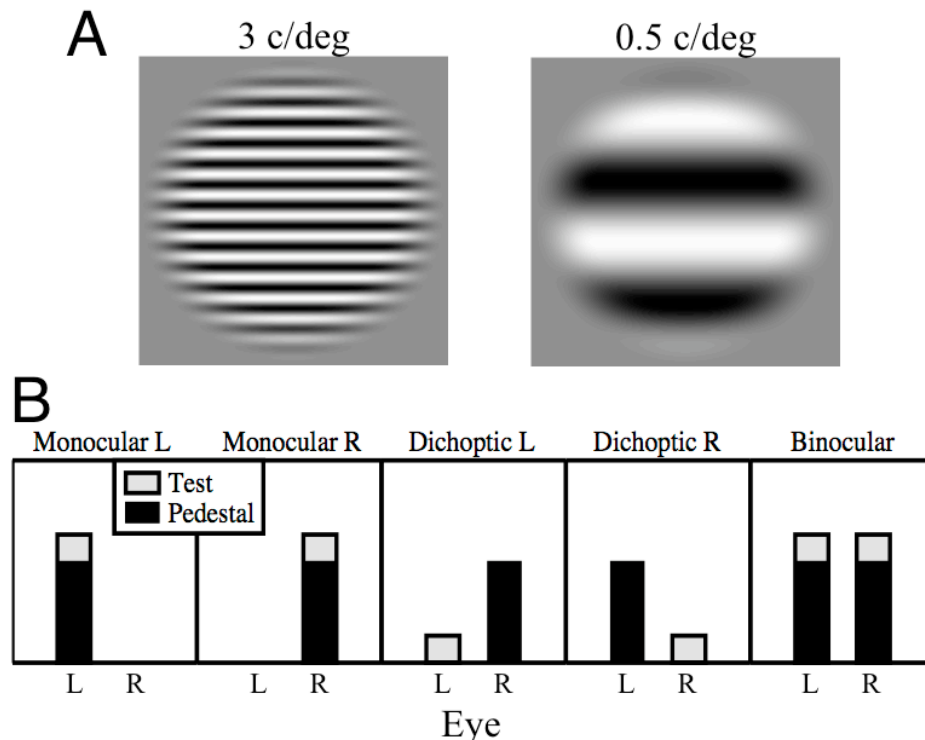

Figure 1: Example stimuli (A) and illustration of the five ocular configurations of test and pedestal (B).

Small vergence movements, or misalignments of the eyes, can cause vertical stimuli to slip out of phase, particularly at high spatial frequencies (Green and Blake, 1981). This problem is exacerbated by stereoscopes that require the observer to actively fuse the images from the two eyes, and for amblyopic observers for whom the eyes are already misaligned. To lessen these problems we used horizontal gratings, ferro-electric shutter goggles (CRS, FE-1) and corrected each observer's strabismus using a prism (see Table 1 for prism strengths and Hood & Morrison, 2002, for a detailed discussion on the use of prisms). The shutter goggles act as a 0.9 log unit neutral density filter and attenuate the luminance of the monitor to around 22cd/m².

Contrast is expressed as a percentage, calculated by $C\% = 100\dfrac{L_{MAX} - L_{MIN}}{L_{MAX} + L_{MIN}}$, where L is luminance, and in decibels (dB), given by $20\log_{10}(C\%)$. Quantitative comparisons between model and data use the root mean square (RMS) error statistic:

$$RMSe = \sqrt{\sum_{i=1}^{n}(model_i - data_i)^2 / n} \qquad (1)$$

where *model* and *data* are the model predictions and empirical data points (in dB), and n is the number of observations (thresholds). Where best fitting model parameters were estimated, a downhill simplex algorithm (Nelder and Mead, 1965) was used to find the parameters which produced the smallest RMS error (in dB).

2.2 Procedure

Observers were seated in a darkened room, 114cm from the display. The goggles were worn on the head and attached using an elasticated strap. Prisms were fixed to the front of the goggles to correct strabismus where appropriate. The prism strength (Table 1) was assessed for each observer before the experiment began so that a pair of nonius lines appeared collinear when viewed with the prism.

We used a two-interval forced-choice procedure (2IFC) where observers used mouse buttons to indicate which of two intervals contained the test-contrast increment. In the monocular and binocular conditions, the test contrast was added to that of the pedestal. In the dichoptic condition, the pedestal contrast was presented to one eye and the test increment to the other eye (see Figure 1B). Stimuli were presented for 200ms, with a 500ms interstimulus interval. The phase of the pedestal was selected randomly from four cardinal values (0, 90, 180 and 270°) on each trial, and was the same for both forced-choice intervals (i.e. the test phase was always the same as the pedestal phase). Each interval was marked by an auditory beep, and auditory feedback was given after each trial to indicate correctness of response. Ten pedestal contrasts were used: 0%, and –10dB to 30dB in steps of 5dB (in percent contrast, these were 0, 0.32, 0.56, 1, 1.78, 3.16, 5.62, 10, 17.78 and 31.62%). Data were gathered in blocks for each pedestal contrast. Within each block, five staircases were randomly interleaved, measuring left and right monocular thresholds, left and right dichoptic thresholds, and a binocular threshold. Observers were not pre-cued as to which eye was being tested on each trial. Each block took around ten minutes to complete, and observers were given the opportunity to rest between blocks. The staircases used a step-size (spacing between contrast levels) of 3dB (a factor of √2), and a 3-down, 1-up rule (i.e. 3 correct responses resulted in a 3dB decrease, and 1 incorrect response resulted in a 3dB increase). Each staircase terminated after 12 reversals in direction.

Observers repeated the experiment four times, apart from DHB and EGF, who performed six and three repetitions respectively. Data were collapsed across session, but analysed separately for each eye using probit analysis (Finney, 1971). DHB also completed the experiment with a 1.5 log unit neutral density (ND) filter in front of the left eye (the magnitude was determined in pilot experiments to produce a marked effect). This reduced the mean luminance by a factor of 32, and was intended to impair contrast sensitivity in the filtered eye.

Observer	Age/Gender	Amblyopia	Prism	Eye	Refraction	Acuity	Detected	Patching	Surgery
ADS	21/F	Right ET, Strabismic	10D	R	Ø	20/125	Age 4	1 year	Age 7
				L	-0.50 DS	20/20			
AR	47/M	Left ET, Strabismic	None	R	Ø	20/20	Age 20	None	None
				L	Ø	20/50			
EGF	56/M	Left ET, Strabismic	1D	R	+3.00/-1.00x90°	20/32	Age 6	1-2 years	None
				L	+3.00/-1.00x40°	20/250			
EMD	43/F	Left ET, Strabismic	3D	R	+0.75 DS	20/16	Age 6	1 year	None
				L	+0.75 DS	20/63			
JL	29/M	Left XT, Strabismic, Mixed	20D (10D each eye)	R	Ø	20/20	Age 4	None	None
				L	+2.50 DS	20/40			
KDJ	22/M	Right XT, Strabismic	3D	R	+1.00 DS	20/50	Age 5	Yes	None
				L	Ø	20/25			
ML	24/F	Right ET, Mixed	3D	R	+1.00/-0.75x90°	20/80	Age 5	2 years	None
				L	-3.25 DS	20/25			
SH	24/F	Left XT, Mixed	6D	R	0.00/-0.50x90°	20/32	Birth	None	None
				L	+4.50/-2.00x90°	20/63			

Table 1: Demographic and clinical details of amblyopic observers. Terminology: ET – esotropia; XT – exotropia; Ø - no refraction necessary. Acuity was measured using a standard logMAR chart.

2.3 Observers

Eight strabismic amblyopes (mean age 33) served as observers. Their clinical and demographic details are shown in Table 1. Normal optical correction was worn, and all amblyopes were psychophysically experienced, but naïve to the purposes of the experiment. All observers were financially compensated for taking part, and were free to terminate the experiment at any time. Procedures adhered to the ethical guidelines of McGill University, where these experiments were carried out. One author (DHB, male, 24) served as a normal control observer and repeated the experiments with a neutral density filter in front of the left eye (see above). DHB is emmetropic, and has good stereoacuity (<8 arc sec, measured using sub-pixel-shifted noise).

2.3.1 Pooling method

The results for the amblyopes were averaged using the pooling method of Burton (1981). For each masking function both dimensions (pedestal and test contrast) were normalized to the observer's appropriate detection threshold. For example, in the dichoptic cases the test contrasts were normalized to detection threshold for the tested eye, and the pedestal contrasts were normalized to detection threshold of the *other* eye.

This process meant that normalized pedestal contrast values were different for each observer, so results were binned across a range of contrasts before averaging (Burton, 1981). The bin size was 5dB (±2.5 dB of the nominal value), equal to the spacing of the pedestal contrasts in the experiment. Pooled data points were removed from the extremes of the masking functions where only one observer contributed to the pool. After pooling, the entire data set was 'de-normalized' so that the axes represent the average sensitivity of the group.

3 Results and Discussion

3.1 Normal observer (DHB)

Results for the normal control observer (DHB) are shown in Figure 2. At both spatial frequencies (panels A, B, D and E) the forms of the masking functions are the same as those reported elsewhere (Meese *et al.*, 2006). In all cases there is facilitation at low pedestal contrasts, and masking at higher pedestal contrasts, producing a classical dipper shape. For the dichoptic conditions (triangles) the facilitation is less and the masking is steeper compared with the monocular (circles) and binocular (squares) conditions.

Binocular summation ratios (SR) were calculated as follows: SR = THRESH$_{mon}$/THRESH$_{bin}$, where THRESH$_{bin}$ and THRESH$_{mon}$ are the binocular and best monocular detection thresholds in percent (pedestal contrast = 0%). Substantial binocular summation was found at detection threshold, as reported previously (Baker et al, 2007b): SR =1.54 at 3 c/deg and SR=1.62 at 0.5 c/deg. The results are well described by the two-stage model (curves in Figure 2A, B, D & E; see Section 4.1 below), with only two free parameters (k and S), as reported in the figure caption. The strong similarity of results across the two spatial frequencies is emphasised by the similarity in the fitted model parameters (S changes from 1.36 (at 3 c/deg) to 1.20 (at 0.5 c/deg), and k is the same in both cases).

The results in Figure 2C & F are for the same normal observer (DHB), but with a 1.5 log unit ND filter in front of the left eye for the 3 c/deg stimulus. The filter substantially reduced the luminance to this eye (by a factor of 32), which increased detection thresholds by about 12dB (a factor of 4). Monocular thresholds and masking in the (normal) right eye were largely unaffected (open circles, Fig 2C). However, the binocular advantage at low mask contrasts was substantially reduced (grey squares, Fig 2C), to the extent that it almost superimposed the monocular function for the normal eye (open circles) and the binocular summation ratio was reduced to 1.16 at detection threshold. There was also a substantial loss of monocular facilitation in the attenuated eye (compare filled and open circles in Fig 2C).
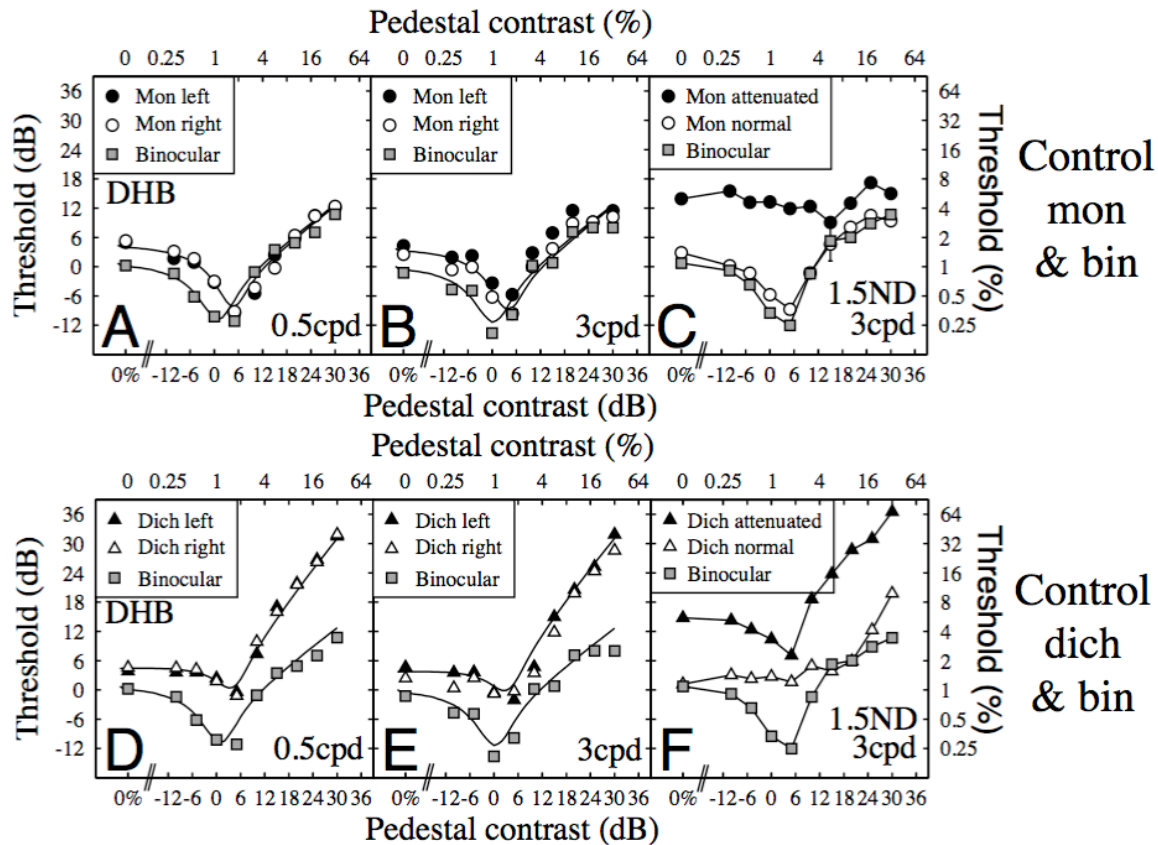
Figure 2: Contrast masking results for a normal control observer (DHB). Results are shown at 0.5 c/deg (A,D) and 3 c/deg (B,E), and also with a 1.5 log unit neutral density filter over the left eye (C,F). To lessen clutter, error bars (determined by probit analysis) are plotted only when they exceed 3dB. The average SE across conditions and panels was 1.1dB. The curves in A, B, D and E are the best fits of the two-stage model, using the parameters from Meese *et al.* (2006), but with *k* and *S* allowed to vary (0.5 c/deg: *k* = 0.21; *S* = 1.36; RMSe = 1.31dB. 3cpd: *k* = 0.21; *S* = 1.20; RMSe = 2.38dB.).

The dichoptic dipper functions were also affected. Dichoptic facilitation was abolished when testing the normal (right) eye, and the masking function shifted rightwards (open triangles, Fig 2F). In the attenuated (left) eye, the dichoptic masking function shifted upwards, and both facilitation and masking remained intact (filled triangles, Fig 2F). Overall, the dichoptic masking in the attenuated ('bad') eye was shifted upwards and to the left of that in the normal ('good') eye (compare open and filled triangles in Fig 2F).

3.2 Amblyopic observers

3.2.1 Monocular and binocular effects

Monocular and binocular results for all eight amblyopes are shown in Figure 3. Detection thresholds and monocular masking for the good eye were similar to those of the normal observer (DHB). However, detection thresholds were between 4 dB and 23dB (factors of 1.6 and 14) higher in the bad eye than the good eye. This was accompanied by an overall decrease in sensitivity at all monocular mask contrasts for the bad eye (filled circles). The monocular dip was typically shallower in the bad eye than in the good eye (see Fig 4), though the main differences across observers were for this condition. For two of the observers (JL and EGF) there were distinct regions of monocular facillitation, and arguably EMD as well. But these three observers also showed the weakest deficits for the null pedestal in the bad eye, suggesting weak amblyopic effects, at least for the spatial frequencies used here.
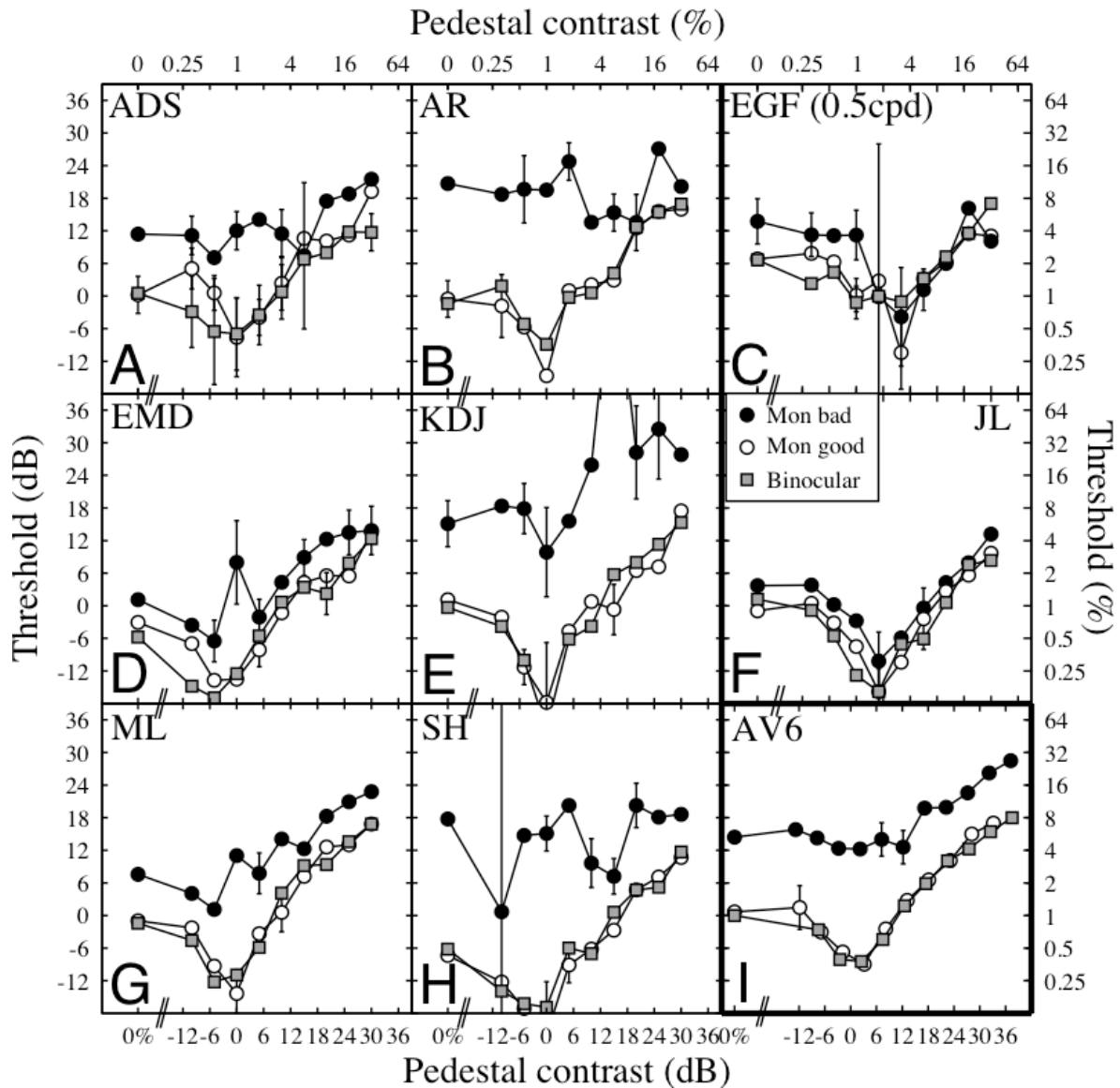
Figure 3: Monocular and binocular contrast masking results for amblyopic observers. 'Good' and 'bad' refer to the eyes that were tested. A-H) Individual observers. I) Average of six observers, using the pooling method described in Section 2.3.1. Error bars are plotted only when they exceed 3dB, and show ±1SE derived by probit analysis for individual observers, or ±1SE of the mean for AV6.

Our strategy for analysis was to compare the form of our average amblyopic data with those of various models (sections 4 below). However, the results for EGF and JL appeared so different from the other observers (particularly for the dichoptic conditions in Fig 5, below) that we excluded them from the averaging to improve the transparency of the main part of our analysis. Nevertheless, we stress that our main conclusions do not depend on this decision, and that the forms of the average data in Figs 3I, 5I and Fig 4 are changed very little when EGF and JL are included (as can be seen by looking ahead to Fig 11B). For simplicity, we refer ro the averages of the six and eight amblyopic observers as AV6 and AV8 respectively. Note that the overall pattern of monocular and binocular masking in AV6 (and AV8) is very similar to that produced by the normal observer with a neutral density filter in front of one eye (compare Figs 2C & 3I).
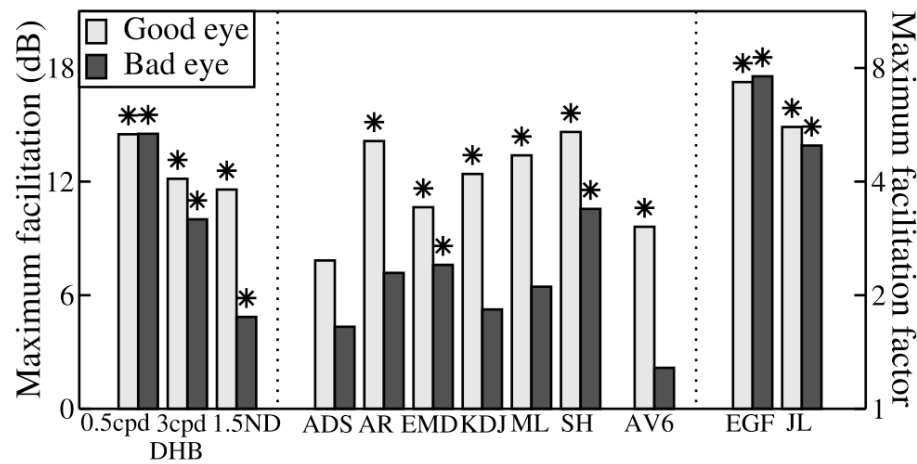
Figure 4: Monocular facilitation in the good eye and bad eye for all observers, and for the pooled average (AV6). Light bars are for the good eye, and dark bars are for the bad eye. For all six observers who contributed to AV6, facilitation was weaker in the bad eye. The level of facilitation for individual observers was calculated as follows. The psychometric functions for each pedestal contrast (including the 0% baseline) were bootstrapped to calculate one-tailed 95% confidence limits (CL). For each observer a short list was made of all the pedestal contrasts that produced a level of facilitation that fell below the CL for the baseline condition. From this shortlist, the largest level of facilitation was selected for which the baseline measure also fell above the CL for the non-zero pedestal contrast. The asterisks mark these levels. When no pedestal contrast was found that met these criteria, the largest facilitatory difference was selected. For these there is no asterisk. Note that the facilitation for AV6 is not the average of the facilitation shown for the six amblyopes, but the facilitation extracted from the AV6 functions in Figure 3I. This was done by bootstrapping the distribution of thresholds that contributed to AV6, and then proceeding as above.

3.2.2 Dichoptic effects

Fig 5 shows the results for dichoptic masking for each amblyopic observer (A-H) and AV6 (Fig 5I). The binocular results are replotted from Fig 3 for comparison. For most of the amblyopic observers the slopes of the dichoptic masking functions were fairly steep, and the levels of masking were fairly high. When testing the good eye (open triangles) there was little or no evidence for dichoptic facilitation for most observers (with the possible exception of AR), though the situation was less clear when testing the bad eye. For two observers (KDJ & ML) there was clear evidence that dichoptic facilitation remains intact, and arguably so for four others (AR, ADS, EMD and EGF), though this translates to only a weak effect in AV6. When testing in the bad eye (filled triangles) masking was shifted upwards and to the left from that when testing in the good eye (open triangles). As in the monocular and binocular conditions, the overall pattern of results was similar to that produced by the normal observer with a neutral density filter in front of one eye (compare DHB in Fig 2F with AV6 in Fig 5I).

3.2.3 Comparison with Harrad and Hess (1992)

Harrad and Hess (1992) hypothesized that amblyopic suppression might have the same cause as dichoptic masking in normal observers (see also Levi et al, 1979). This predicts that dichoptic masking functions for the two eyes should superimpose when plotted on threshold-normalized axes and that both functions should have a log-log slope of about unity (Weber's law; see Legge, 1979). But this prediction was not borne out for the majority of their observers for whom the slopes of the masking functions differed markedly between the eyes. For strabismic amblyopes, when the test and pedestal were presented to the amblyopic and normal eyes respectively, masking was stronger than in normal observers. When pedestal and test eyes were reversed, masking was substantially weaker than in normals, and sometimes absent altogether. Harrad and Hess (1992) concluded that strabismic amblyopes suffer greater suppression of the amblyopic eye by the normal eye, and weaker suppression in the opposite direction, compared with normals.
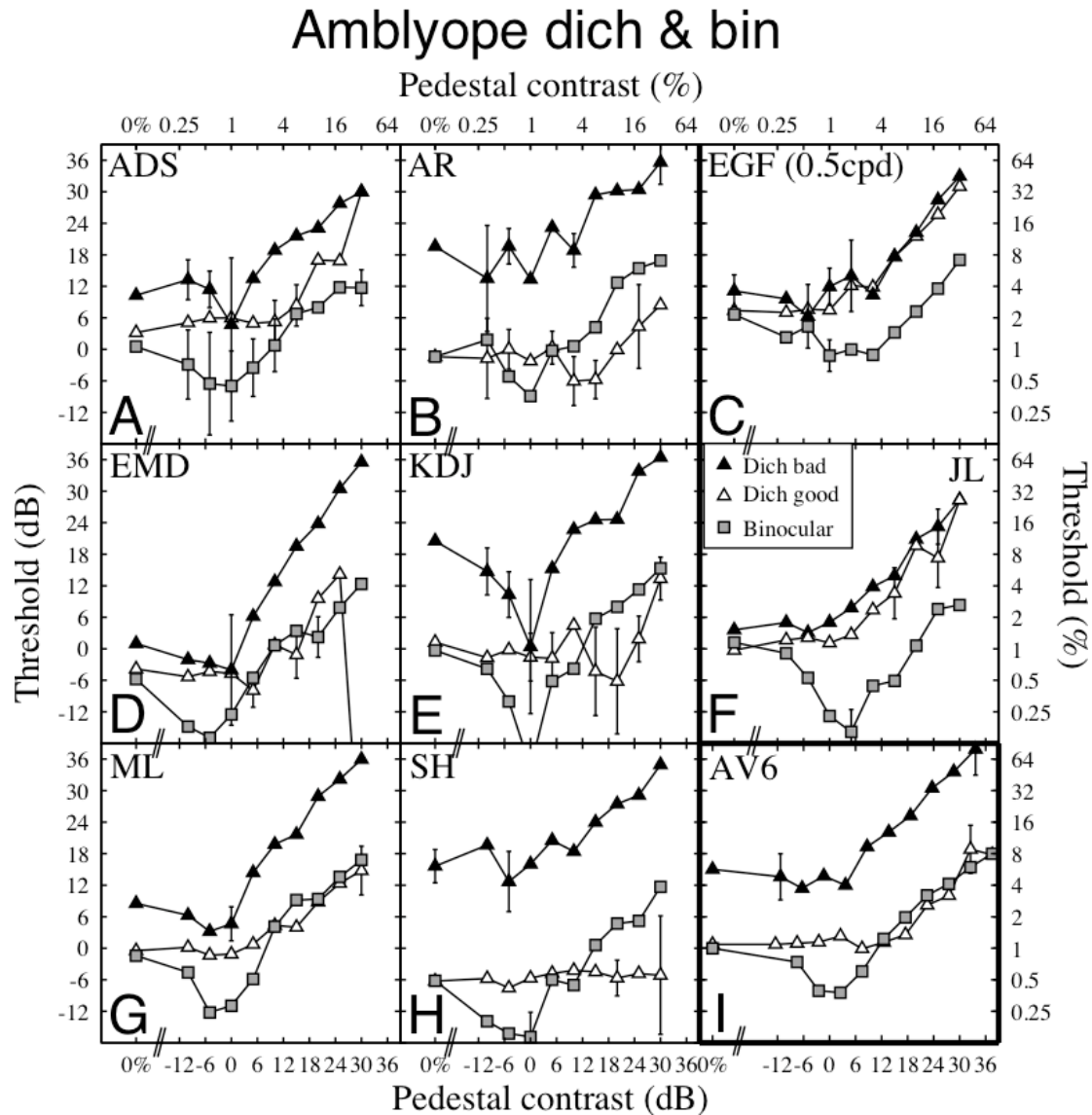
Amblyope dich & bin

Figure 5: Dichoptic and binocular contrast masking functions for amblyopic observers. The binocular data are replotted from Fig 3. Panel layout and other details are the same as for Figure 3.

One of the main aims of the empirical part of the present study was to characterise contrast vision in strabismic amblyopia by measuring masking functions for the five conditions in Figures 3 and 5. However, we also wanted to compare these with the dichoptic masking functions measured by Harrad and Hess (1992) for the same clinical condition. To facilitate this we performed a more detailed examination of the dichoptic masking.

The dichoptic results are replotted on normalized axes in Figure 6. The oblique lines are the contours of contrast equality between the two eyes, normalized to detection threshold. In normal observers, dichoptic masking functions sit just below this line (e.g. Baker & Meese, 2007), meaning that the contrast needed for detection is typically just a little less than the contrast of the pedestal. For amblyopic observers, Figure 6 shows that when testing the bad eye (solid triangles), masking can be less severe than normal but that when testing the good eye (open triangles) the levels of masking are similar to or greater than normal. This contrasts with the strabismic results of Harrad and Hess, where masking was either more severe in the bad eye, less severe in the good eye or both of these. We return to this discrepancy in the Discussion.
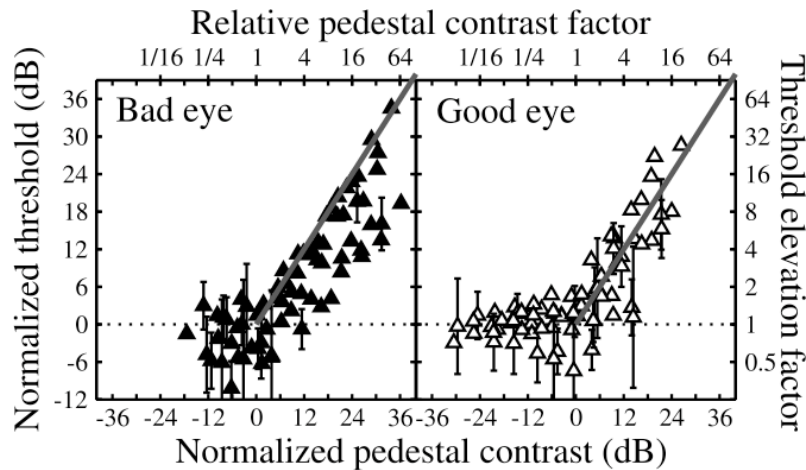
Figure 6: Normalized dichoptic masking results for the group of eight amblyopic observers. 'Good' and 'bad' refer to the eyes that were tested. The oblique line is the line of equality between the normalized pedestal and test contrasts and has a slope of unity (Weber's law). Overall, this shows that masking is more severe when testing in the 'good' eye than in the 'bad' eye. Points below the horizontal dotted line indicate dichoptic facilitation.

Another effect found by Harrad and Hess (1992) was that for some observers, the slopes of the dichoptic masking functions were unusually steep in the bad eye and/or unusually shallow in the good eye. The slopes of dichoptic masking for the present study are shown for each amblyopic observer and for the normal control observer (DHB) in Table 2 (see caption for methodological details). There is much variation across eye and between observer, but for none of our amblyopes was there a marked effect in the expected direction for both eyes, though several amblyopes (e.g. EMD, ML, SH) showed one or the other of the effects. On the other hand, several amblyopes showed effects in the opposite direction: unusually steep masking in the good eye (KDJ) or shallow masking in the bad eye (AR and SH), indicating heterogeneity of this aspect of the results. Harrad and Hess also found some marked individual differences in the strengths of the effects amongst their group of strabismic amblyopes.

Finally, our normal observer showed normal dichoptic masking (a slope of about unity) when simulating the effects of amblyopia with a neutral density filter. Without the filter (top two rows in Table 2), the masking slopes for DHB were slightly steeper than might be expected (unity) because of the initial acceleration out of the 'dip' region (see Fig 2D, E & F) that contributes to the analysis here; DHB's slopes were much closer to unity in the higher parts of those functions (not shown).

3.2.4 Dichoptic facilitation and binocular summation

Dichoptic facilitation was found for several of our observers (points below the horizontal dotted line in Figure 6), and in some cases was quite distinct when testing the bad eye (Fig 5). This is of particular interest because it seems likely that dichoptic facilitation is a consequence of excitatory binocular summation (see Meese *et al.*, 2006; Baker & Meese, 2007), suggesting that summation remains intact in the amblyopic visual system (Baker *et al.*, 2007b). This conclusion might seem at odds with the findings (here and elsewhere) that empirical estimates of binocular summation ratios (defined in section 3.1) in amblyopic observers are much less than for normal observers (see Table 2). However, in general, we do not attribute this deficit to dysfunctional neural convergence between the eyes, but to a loss of benefit from the insensitive eye. This aspect of the results is the subject of a companion paper (Baker *et al.*, 2007b) where we provide a detailed analysis of the data from six of the amblyopic observers here (EGF and SH were not available for the further testing in that study), as well as three normal controls, each with and without a neutral density filter. One important outcome of that study is that binocular summation of horizontal gratings was within the normal range for all observers when contrasts were normalised across the eyes (see also Section 1.3).

| | Dichoptic slopes | | |
Normal observer	Left/attenuated eye	Good/normal eye	Bin sum ratio
DHB 0.5cpd	1.27	1.26	1.62
DHB 3cpd	1.35	1.23	1.54
DHB 3cpd ND	1.08	1.08	1.16
Amblyopic observer	Bad eye	Good eye	Bin sum ratio
EGF	1.12	0.93	0.98
JL	0.74	0.88	1.03
ADS	0.78	1.16	1.02
AR	0.66	0.78	1.28
EMD	1.27	1.06	1.25
KDJ	1.05	1.95	1.14
ML	0.98	0.54	1.06
SH	0.59	0.04	0.88
AV6	0.82	0.69	1.08
Model observer	Bad eye	Good eye	Bin sum ratio
Multiplicative noise (Fig 10A & 11B)	0.85	1.04	1.00
Additive noise (Fig 11D)	1.06	1.04	1.08

Table 2: Dichoptic masking slopes and binocular summation ratios for all observers and conditions. For completeness, the bottom part of the table is for the two most successful models described later in the text (Sections 4.2.4 and 4.4). Binocular summation ratios were calculated as descibed in Section 3.1. The dichoptic slopes were calculated by performing linear regression on the upper limb of each dichoptic function (using dB units). This was defined as the region which extended from the pedestal contrast that produced the greatest sensitivity to the test-increment (i.e. the lowest point in the 'dip'). In several instances (9 out of 28), however, we judged that more representative measures could be made as follows. Left/bad eye: EGF 6th point from left, AV6: 5th point from left. Right/good eye: DHB, 3 cpd, 5th point from left; DHB 3 cpd with ND filter, 7th point from left; EGF, 6th point from left; ADS, 6th point from left; EMD highest mask contrast omitted; Model observers, 7th point from left. Note also that the slopes for AV6 are not the average slopes for the six amblyopes, but those extracted from the AV6 functions in Figure 5I.

In Fig 5, there are some notable differences between observers for dichoptic masking when testing in the good eye (open triangles). For most observers (ADS, AR, EMD, KDJ & ML), the level of masking was fairly similar to that in the binocular condition (grey squares), but for one observer (SH) there was no masking at all. This is probably because sensitivity was so low in the bad eye (see Fig 5H) that the pedestal was not an effective mask, even at the highest pedestal contrasts. However, we note that the threshold deficits for AR and KDJ are comparable to that of SH, yet some dichoptic masking is also evident for those observers. For two other observers (EGF & JL), dichoptic masking was substantial and similar for both eyes. This is probably to be expected if these two observers suffer only weakly from their condition as we suggested above.

More generally, we note that the main individual differences are found when testing the bad eye in the monocular case (filled circles, Fig 3), but the good eye in the dichoptic case (open triangles, Fig 5). This suggests that the origin of the individual differences is in the bad eye but before interocular suppression, so that it can influence the dichoptic case. Of the model lesions that we consider in section 4, those that meet with success are consistent with this view.

3.3 Summary of main findings: Four criteria for a successful model

In section 4 (below) we attempt to shed light on the amblyopic deficit by exploring the effects of various types of lesion on the two-stage gain control model of contrast discrimination (Meese et al, 2006). However, we first list the criteria derived from our amblyopic results against which the models should be judged. These characteristics are also consistent with the results from our normal observer with the ND filter (Fig 2).

C1. When only one eye is tested (monocular or dichoptic), sensitivity is worse in the bad eye than the good eye for all mask contrasts (Figs 3 and 5).

C2. Binocular and monocular dipper functions superimpose in the good eye (Fig 3).

C3. Monocular masking functions have a normal dipper shape in the good eye, but facilitation is reduced or absent in the bad eye (Figs 3 and 4).

C4. Dichoptic facilitation survives when testing the good eye, but possibly not when testing the bad eye (Figs 5 and 6).

C1, C2 and C3 represent clear results seen in AV6 (and AV8 – Fig 11B) and most of the amblyopic observers (the possible exceptions being EGF and JL). *C4* is marginal and set in italics as a reminder of this. This result is less consistent across observers, though dichoptic facilitation in the bad eye is clearly evident in KDJ, ML and the normal observer with the ND filter.

The variability in results meant that we had no clear prediction for the slopes of dichoptic masking (Fig 5 and Table 2), though a model predicting a slope markedly greater than unity or less than ~0.7 might be a cause for concern. This does not form a formal part of our rejection criteria, but receives further comment below where appropriate. The slopes of monocular and binocular masking appeared fairly normal in most cases (~0.6 for AV6 and AV8) and did not constrain our model selections.

4 Modelling

4.1 Two-stage model of contrast gain control

We first describe the two-stage model of Meese *et al.* (2006) and then devise various ways in which the model can be 'lesioned' to try and account for the abnormalities of the amblyopes and DHB with the neutral density filter.

The two-stage model was initially developed for normal observers and for the same three conditions as studied here (monocular, binocular and dichoptic masking). The model has two distinct stages of contrast gain control, one before and one after binocular summation. Stage 1 includes divisive interocular suppression, and for the left eye is given by:

$$resp_L = \frac{C_L{}^m}{S + C_L + \omega_R C_R}, \tag{2}$$

where C is stimulus contrast (in percent) in the left (L) and right (R) eyes, and S and m are model parameters. This is followed by binocular summation

$$binsum = \frac{C_L{}^m}{S + C_L + \omega_R C_R} + \frac{C_R{}^m}{S + C_R + \omega_L C_L}, \tag{3}$$

which is the linear sum of Eq 2 and an equivalent expression for the other eye. The interocular weights (w_L and w_R) are set to unity for normal observers (Meese *et al*, 2006).

The second gain control stage of the model is given by:

$$resp = \frac{binsum^p}{Z + binsum^q}, \tag{4}$$

where p, q and Z are model parameters, and *binsum* is the output of equation 3. We discuss how these parameters might be interpreted in Baker, Meese & Georgeson (2007a). Threshold is reached when the difference between the response in the null and test intervals exceeds some criterion level. Thus, we have:

$$k = resp_{ped+test} - resp_{ped}, \tag{5}$$

where k is a model parameter, and is proportional to the standard deviation of late additive noise. The full model has six free parameters: m, S, p, q, Z and k. To reduce the number of degrees of freedom, several of these were fixed at values derived from Meese *et al.* (2006). These were: $m = 1.28$, $p = 7.99$, $q = 6.59$, $Z = 0.076$. This is reasonable because the parameters p, q and Z are placed at the second stage in the model where they affect both eyes and determine the form of the monocular and binocular masking functions. Since monocular functions in the good eye are normal, it seems likely that these parameters are not affected by amblyopia. We also had no *a priori* reason to suppose that the value of m would be affected by amblyopia. This was confirmed by preliminary tests of the model (not shown). For the normal observer, the two free parameters k and S control sensitivity and the placing of the dipper region, and were set to the values reported in the caption of Fig 2 by the fitting procedure. For further details

and discussion of this model see Meese et al (2006) and Baker, Meese & Georgeson (2007a).

4.2 Models of amblyopia

Although there are marked differences between the amblyopic observers in this study, many of these are of magnitude rather than kind. Our approach is to progress through various 'lesions'[2] in the model with the aims of (a) describing the main trends in the average amblyopic data (AV6 in Fig 3I & 5I) and (b) documenting the behaviours of various potential models of amblyopia. We then consider how individual data sets (specifically, JL and EGF) might be described by alternative treatments. We 'lesioned' the model in four different ways: (i) by increasing interocular suppression, (ii) by ablating the binocular pathway, (iii) by inserting attenuators, and (iv) by including additional sources of noise.

4.2.1 Abnormal interocular suppression?

One abnormality that has been advanced to explain the perceptual losses in amblyopia is unusually high levels of interocular suppression of contrast from the good eye onto the bad (Holopigian, Blake & Greenwald, 1988; Harrad, Sengpiel & Blakemore, 1996; Agrawal et al., 2006). In the two-stage model this can be implemented by adjusting the weights of divisive interocular suppression on the denominator of stage 1 (equation 2). Figure 7 shows the effects of various weight combinations of interocular suppression across the eyes. The solid curve (replicated in each panel) shows normal behaviour where both suppressive weights are unity. Dashed and dotted curves show behaviour when testing the left and right eyes respectively, and when the interocular weights are adjusted. Different patterns of weights can vary the overall strength of masking quite substantially, making it greater (Fig 7C) or weaker (Figs 7A, B & D). However, perhaps surprisingly, the magnitude of masking remains similar across the two eyes, even when the weights differ by a factor of 10 (Fig 7D). We were unable to find any combination of model weights that was able to tease these functions apart substantially while at the same time producing masking functions that resembled the form of the data. In other words, with this manipulation alone we could not describe our finding that dichoptic masking can be

very different in the two eyes (C1).

The reason for the counterintuitive behaviour of this model (Fig 7) owes to the dual contribution to dichoptic masking from interocular suppression and binocular combination (Baker & Meese, 2007; Meese et al., 2006). The less obvious of these two factors is that interocular suppression from the *test* on the *pedestal* contributes to a reduction in overall output after binocular summation between pedestal and test. (Recall from section 3.2.3 that this effect will be substantial, because normal dichoptic masking thresholds are nearly as high as the pedestal contrast). Thus, increasing the weight of interocular suppression from the pedestal increases the direct effect of interocular suppression on the test, but when test and pedestal eyes are swapped it also increases the indirect effect of the test on the pedestal. As the two effects have similar consequences the dichoptic masking functions for the two eyes (Fig 7) are affected in similar ways. The only way to bypass the 'indirect effect' of masking (the consequence of the test suppressing the pedestal) is to compromise binocular summation. In the next section we achieve this by inserting attenuators into the model, and in section 4.2.3 we consider complete binocular ablation.
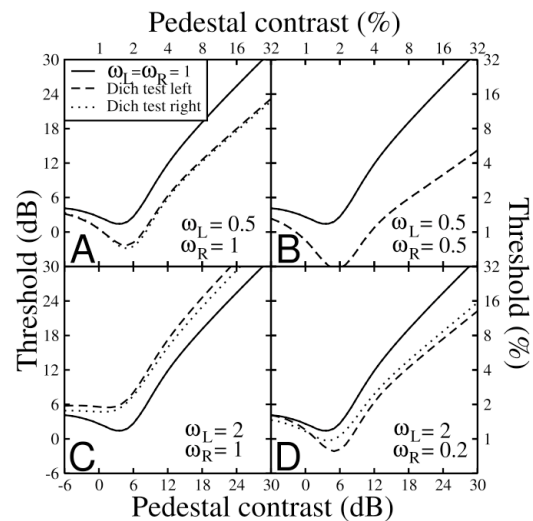

Figure 7: Effects on dichoptic masking of varying the weight of interocular suppression in the model. The solid line shows normal dichoptic behaviour ($\omega_L=\omega_R=1$), and each panel contains model predictions for different combinations of dichoptic weights in the left (dashed curves) and right (dotted curves) eye. A) One of the weights is halved. B) Both of the weights are halved (the two functions superimpose here). C) One of the weights is doubled. D) One weight is doubled; the other is reduced by a factor five.

---

[2] We take a broad interpretation of the term 'lesion', and use it to mean any form of (gross) corruption applied to the model originally used for normal observers.

4.2.2 Attenuator model

One way to model amblyopic threshold elevation is to insert an attenuator in the model's amblyopic eye. A fixed attenuator divides its input by a constant amount, the magnitude of which is an additional free parameter (A). We first considered an attenuator placed before stage 1. In this case, the signal in the bad eye's channel is equal to the input contrast divided by a constant:

$$C_{OUTPUT} = \frac{C_{INPUT}}{(1+A)}. \qquad (6)$$

C_{OUTPUT} then replaces C for the bad eye channel in equation 3. The remainder of the model and the values of its fixed parameters, are as described in section 4.1 and the caption of Fig 2 ($S = 1.20$; $k = 0.21$).

The behaviour of this model is shown in Figure 8A. The attenuator (set to $A = 2$ to achieve reasonable comparisons by eye) raises detection threshold in the affected eye and shifts the monocular and dichoptic masking functions for that eye upwards and to the right. The dip regions for both functions remain intact, and the slopes of the upper regions remain unchanged. The binocular function is also elevated, and superimposes the monocular function for the good eye. This behaviour produces only a marginal pass for C1 (the monocular masking in the bad eye is probably too close to that in the good eye) a pass for C2, and possibly *C4*, but fails badly on C3 because monocular facilitation survives in the bad eye.

We also considered two other locations for the attenuator. Placing it at stage 1 is equivalent to adjusting the saturation constant, S in the bad eye. Placing it after stage 1 involves treating C_{INPUT} in Equation 6 as the output of stage 1 (Equation 2) and replacing the first term on the right-hand side of Equation 3 with C_{OUTPUT} in Equation 6. The strength of attenuation was adjusted in each of these positions to produce an amblyopic loss of sensitivity of about 12dB at detection threshold, consistent with the results (Figs 3 and 5). However, in neither case did this improve matters against C1, and when the attenuator was at stage 1 it made matters worse against C2. It also made the slopes of the dichoptic masking functions unusually steep: slope = 1.42 for the good eye for attenuator at stage 1, and slope = 1.75 for the bad eye for attenuator after stage 1. These are steeper than most of the empirical dichoptic masking functions here (Table 2), though in the second case, broadly consistent with some of the results from Harrad and Hess (1992).

For large values of A at either of these alternative positions the binocular function was elevated above the monocular one, producing 'binocular inhibition'. Although there are empirical reports of this phenomenon (Pardhan & Gilchrist, 1992; Hood & Morrison, 2002) this was not seen for our observers here (with the possible exception of JL; Fig 3F & 5F). In sum, of the three attenuator positions considered, the early attenuator location achieved the best overall results.
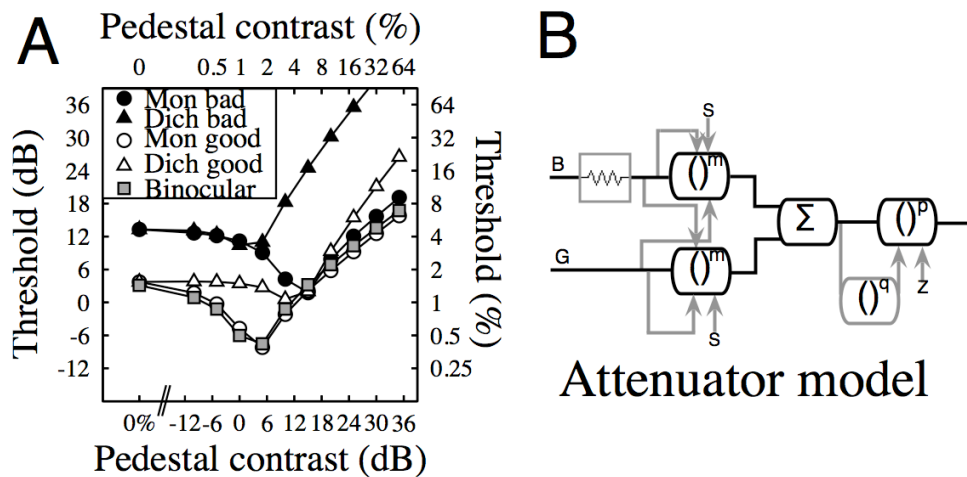

Figure 8: Behaviour (A) and architecture (B) for the attenuator model.

4.2.3 No binocular summation?

Another candidate model of amblyopia is one in which binocular summation is ablated, leaving the amblyopic system with two channels, each with monocular drive but subject to interocular suppression (e.g. Meese & Hess, 2004). When the two-stage model is modified this way, the response of the left-eye channel is given by:

$$resp_L = \frac{\left(\dfrac{C_L{}^m}{S + C_L + \omega_R C_R}\right)^p}{Z + \left(\dfrac{C_L{}^m}{S + C_L + \omega_R C_R}\right)^q}, \tag{7}$$

and there is a corresponding expression for the right eye. We also insert an attenuator in the amblyopic eye (see previous section)—arbitrarily designated the left eye—so that the output of equation 6 forms the input (C_L) to equation 7. The final model response is determined by the channel with the largest output (a peak-picker or MAX operator), such that,

$$output = MAX[resp_L, resp_R]. \tag{8}$$

The architecture of this model is shown in Fig 9A and its behaviour in Figure 9D. Not surprisingly, when binocular summation is removed from the model there is no benefit of two eyes over one at threshold. In fact, interocular suppression means that the binocular function (squares) is elevated slightly above the monocular function for the good eye (open circles). This offers another plausible architecture for binocular inhibition (Hood & Morrison, 2002; Pardhan & Gilchrist, 1992) but does not describe the amblyopic observers here, failing against C2, C3 and *C4*. Furthermore, the model passes only marginally against C1 (the upper limbs of the monocular masking functions are too close together).

A further possible problem area for this model is with dichoptic masking. As described in section 3, it was difficult to summarise this phenomenon in our empirical results, but the model in Fig 9A appears to assert its influence too soon (compare Fig 9D and Fig 3I). The reason dichoptic masking is so strong in this model is because the test eye must overcome the interocular suppression from the pedestal *and* exceed the activity in the pedestal eye to win out with the MAX operator.

The severity of dichoptic masking is reduced by setting the weight of interocular suppression (ω in equation 7) to zero. In this case, the monocular response for the left eye becomes:

$$resp_L = \frac{\left(\dfrac{C_L{}^m}{S + C_L}\right)^p}{Z + \left(\dfrac{C_L{}^m}{S + C_L}\right)^q}, \tag{9}$$

and there is a similar expression for the right eye. As above, an attenuator is included so that the output of equation 6 forms the input (C_L) to equation 9, and the final output is determined by a MAX operation across eyes (equation 8).

This version of the model has entirely independent monocular channels: excitatory and inhibitory binocular interactions have both been removed (see Figure 9B). This reduces dichoptic masking to more appropriate levels (Figure 9D) and correctly predicts the superposition of binocular and monocular (good eye) functions (so it passes C2). However, this model is marginal with C1 (as above), and fails C3 and *C4* because monocular facilitation survives in the bad eye, and there is no dichoptic facilitation.

In a final attempt to salvage the general idea that binocular summation is ablated, we tried another version in which we modified the output stage (Fig 9C). The observer was assumed to monitor only the eye containing the test (i.e. *output = resp_L* or *output = resp_R*, as appropriate) and interocular suppression remained intact, because without it there could be no dichoptic masking. Model behaviour is shown in Fig 9F. One problem with this model is that the slope of dichoptic masking is arguably too shallow (~0.6), because the normal dual contribution of dichoptic masking has been removed (Meese & Hess, 2004; Baker & Meese, 2007). But in any case, it fails against the facilitation criteria of both C3 and *C4*.
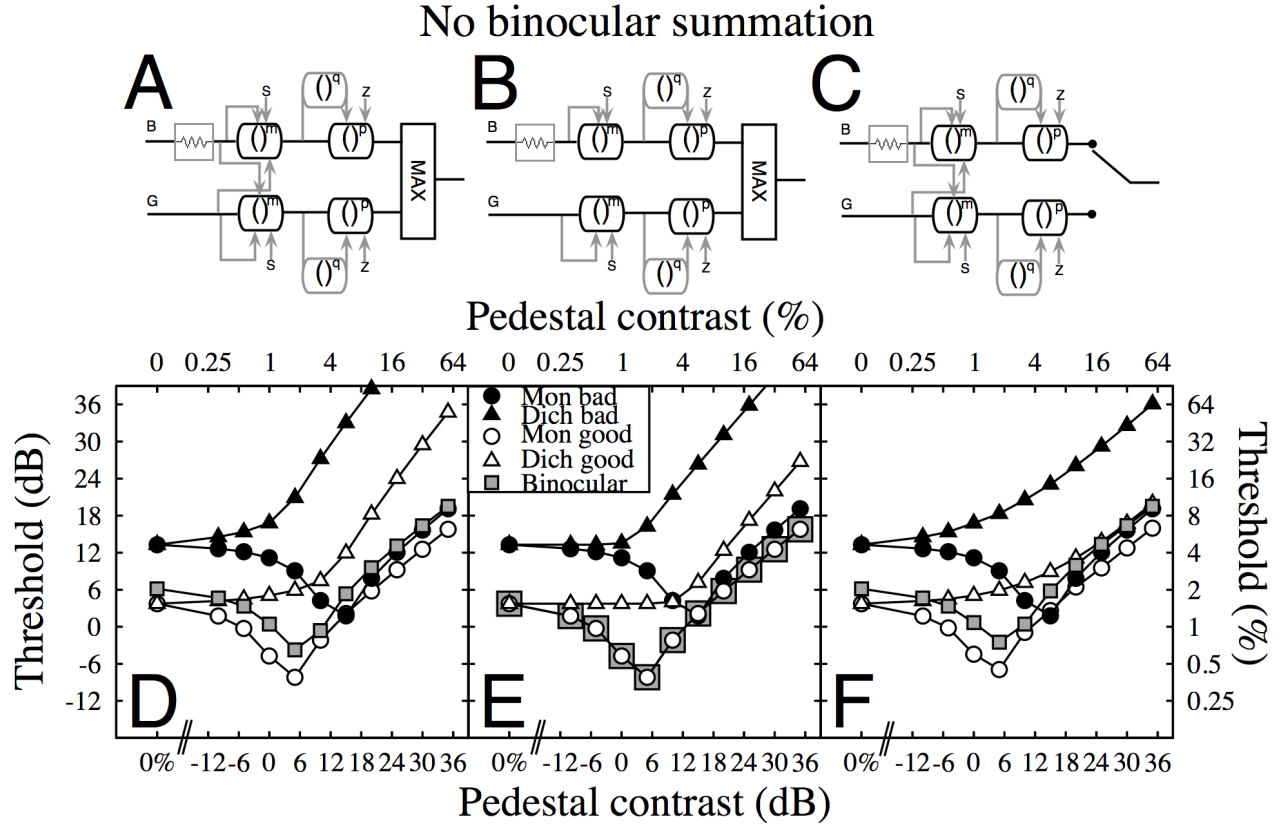
No binocular summation

Figure 9: Architectures (A - C) and behaviours (D - F) of models with an amblyopic attenuator and no binocular convergence, with (A, C, D, F) and without (B, E) interocular suppression. Parameters: $k = 0.21$, $S = 1.20$, $A = 2$ for all panels.

Finally, we note that the absence of binocular convergence in all of the models considered here means that they cannot produce binocular summation at threshold, even when the monocular contrasts are normalized to each eye's sensitivity (see section 1.3). In our companion paper (Baker *et al*, 2007b), however, we show that this does happen for a group of nine amblyopes (including six of those here) and three normal observers with an ND filter in front of one eye. This makes the architectures in Figure 9 all the more unlikely as a general scheme.

4.2.4 Noise model

The (early) attenuator model (Fig 8, section 4.2.2) captures many of the important features of our results. However, several subtle amblyopic effects are missed, most notably, the reduction of monocular facilitation in the amblyopic eye (C3), and a marked separation between the monocular dipper handles. We now account for these effects by injecting noise into the amblyopic eye of the attenuator model. On a trial-by-trial basis, this 'blurs' the location of the dip, making it broader and shallower. We implemented this 'early' noise

stochastically by making the saturation constant (*S*) in the amblyopic eye noisy:

$$S_{AMB} = S * abs(G_\sigma), \qquad (10)$$

where the full-wave rectification of the noise prevents the expression from going negative. The Gaussian noise has standard deviation σ. We also used a stochastic noise source (G_l) to simulate the late additive noise that was previously represented by the deterministic parameter k (equation 5). We set $s = 3$, $A = 2$ (as before), and $l = 0.2$ (from SDT, this is equivalent to our earlier value of $k = 0.21$ at the 75% correct point in the deterministic model). The model was run on a trial-by-trial basis using the same staircase procedure as that used in the experiments, and independent samples of noise were drawn for each source on each 2IFC interval. The simulated (model) observer chose the interval with the larger response on each trial. This entire procedure (simulated experiment) was repeated 2000 times to generate the average model curves plotted in the figures.
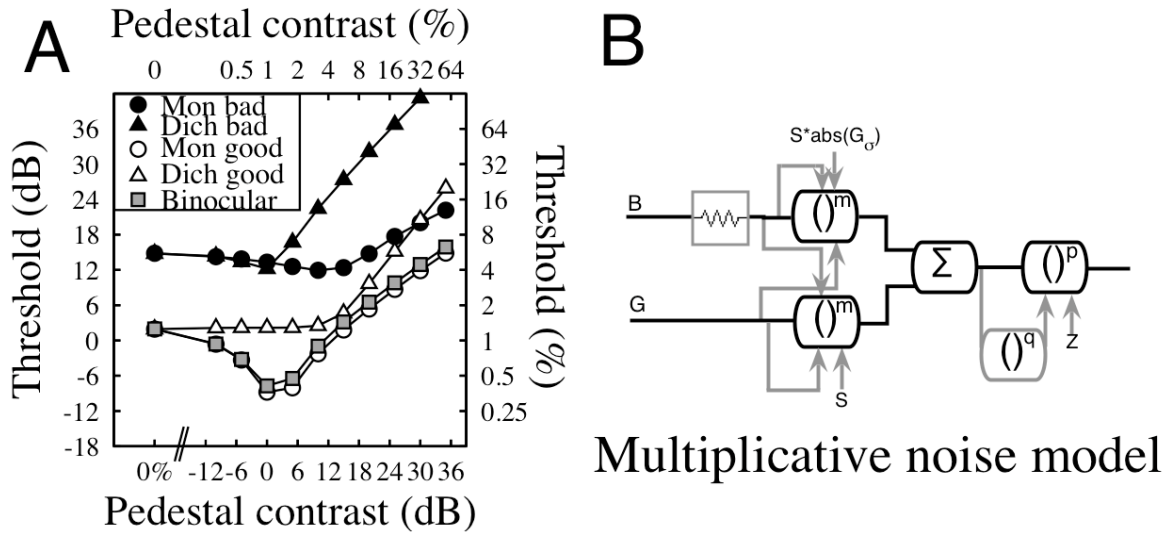
Figure 10: Behaviour of the multiplicative noise model (A) and schematic illustration of its architecture (B). This is identical to the early attenuator model described in section 4.2.2, but with a full-wave rectified stochastic noise source applied to the saturation constant (S) in the bad eye. This noisy saturation constant deemphasises the dip region of the bad eye's monocular function, and reduces dichoptic facilitation in the good eye.

The behaviour of this version of the model is shown in Figure 10A. It shares the successes (e.g. C2) of the early attenuator model, owing to its similar archtecture, but the additional noise captures several nuances in the amblyopic data that did not emerge before. First, the monocular dipper handles (circles) do not fall close together (as they do in the early attenuator model) but are widely separated, providing a better pass for C1. Second, the monocular facilitation in the amblyopic eye is dimished (solid circles), though it remains intact in the good eye and for binocular stimulation (open circles and grey squares), thereby passing C3. Third, dichoptic facilitation in the good eye is abolished (open triangles), though its vestige remains in the bad eye (solid triangles), providing a better pass for *C4*. This is the first model to pass all four of our criteria oulined in section 3.3. In other words, we have been able to describe our main amblyopic effects by corrupting the two-stage model of contrast gain control with just two new parameters: the attenuator parameter, *A* and the noise parameter *s*. Note that both of these 'amblyopic' components are placed in the amblyopic eye, before binocular summation. Placing either of them after binocular summmation does not work because they influence all five masking functions. Although influences in the non-amblyopic eye have been reported using a very different paradigm (Levi & Klein, 2003), there is no evidence of that here; the monocular dipper functions are completely normal in the good eye for all of our observers.

4.3 Individual differences

Our preferred model of the average amblyope (AV6) in the present study is the attenuator model with early noise in the bad eye. This provides a good account of both gross and subtle aspects of the amblyopic data as well as the results form the normal observer with the neutral density filter (it passes C1, C2, C3 and *C4*). However, the masking functions for EGF and JL are distinct from AV6 in two main respects. First, there is an approximate superposition of the monocular (circles in Fig 3C & F) and dichoptic (triangles in Fig 5C & F) masking functions for the two eyes. This is presumably due to the fact that the loss of sensitivity in the bad eye is not as severe as it is for the other observers, and so might not represent a difference in kind. In fact, these two observers are less abnormal than the other amblyopes (at the spatial frequencies tested), though both have a loss of contrast sensitivity in the bad eye, and neither show a binocular advantage at low mask contrasts. We found that our model provided a fair description of these observers by reducing the level of attenuation and monocular noise, but we could not account for their loss of dichoptic facilitation this way (triangles, Fig 5C and 5F). However, the similarity between these data sets and some of the other models means that those models might survive as accounts of some amblyopic observers. For example, EGF and JL are consistent with an absence of binocular summation (Fig 9; note that a smaller attenuator would reduce the separation between the good and bad eye functions). However, on this last point, evidence from our

companion paper (Baker et al, 2007b) shows that binocular mechanisms are intact for JL. EGF was not available to take part in that study, so his binocular status remains unknown.

4.4 Normal observer, AV6, AV8 and alternative noise models

Our noise model (Fig 10B) involves an early attenuator and a noisy saturation constant (S) at stage 1 of the model. It provides a good account of our amblyopic data (AV6) and, owing to their similarity, the results of the normal control observer (DHB) with the neutral density filter. We replot these empirical data showing all five masking functions on common axes in Fig 11A and Fig 11C for direct comparison against the model in Fig 11D (replotted from Fig 10A). This model involves a form of signal dependent (multiplicative) noise, because as the contrast in the bad eye increases, the variance of the contrast response at the output of stage 1 also increases. The main reason for choosing this form of noise was because it separated the monocular masking functions in the two eyes at high mask contrasts, as we found in AV6 (compare the circles in model and data in Fig 11A & D). Levi & Klein (2003) and Levi *et al* (2007) have also presented data and arguments in favour of a signal dependent component in amblyopic noise. However, we also tried another arrangement in which additive Gaussian noise was combined with the signal at the input to stage 1 and then half-wave rectified, to prevent negative signals[3]. The initial stage of the amblyopic eye becomes:

$$C_{OUTPUT} = \frac{MAX[0, C_{INPUT} + G_\sigma]}{(1 + A)}, \qquad (11)$$

replacing equations 6 and 10 (Parameters: $A = 2$, $\lambda = 0.2$, $\sigma = 4$). This produced the model behaviour in Fig 11E, and is very similar to that shown in Fig 11D, except that the dipper handles for the two monocular masking functions fall closer together. Parameter manipulation (A, λ, and σ) cannot pull them apart again without otherwise distorting the forms of the masking functions. Curiously though, this provides a more appropriate comparison with AV8 (Fig 11B), since the main effect of including EGF and JL in the average is to pull the two

monocular dipper handles closer together. Given the variability in our data, the general similarity between the models and, no doubt, the various other ways in which noise could be implemented, we do not make any claims about whether the amblyopic noise here is additive or multiplicative. However, we do note that it is well-modelled using multiplicative noise.

Finally, we wondered whether the attenuator was strictly necessary in these noise models. To test this we reran both types of noise model with $A=0$, but for neither model (nor a combination of the two), could we find parameter values (of *s* and *l*) that allowed the model to pass all four criteria (C1 – *C4*).

5 General Discussion

To investigate amblyopic contrast vision at threshold and above we performed pedestal masking experiments for binocular, monocular and dichoptic presentations of horizontal pedestals and test gratings in eight strabismic amblyopes. Unlike results from normal observers, we found little or no binocular advantage around detection threshold, and contrast sensitivity was compromised when testing in the bad eye across the full range of pedestal contrasts (for monocular and dichoptic masking). However, the form of the monocular dipper function was normal when testing the good eye, as was the binocular dipper function. The forms of the dichoptic masking functions were also fairly normal for both eyes, though their slopes varied somewhat, and normal dichoptic facilitation was absent when testing the good eye. The function with greatest abnormaility was the monocular masking function when testing in the bad eye. In most cases, thresholds were severely elevated (Fig 3), facilitation (the 'dip') was much diminished (Fig 4), and the data were generally much less tidy than for the other conditions (Fig 3).

---

[3] Strictly speaking, this implementation of additive noise is signal dependent because the half-wave rectification decreases the effective variance of signal plus noise at very low signals. When the signal is twice the standard deviation of the additive noise or above, the variance is essentially independent of signal strength.
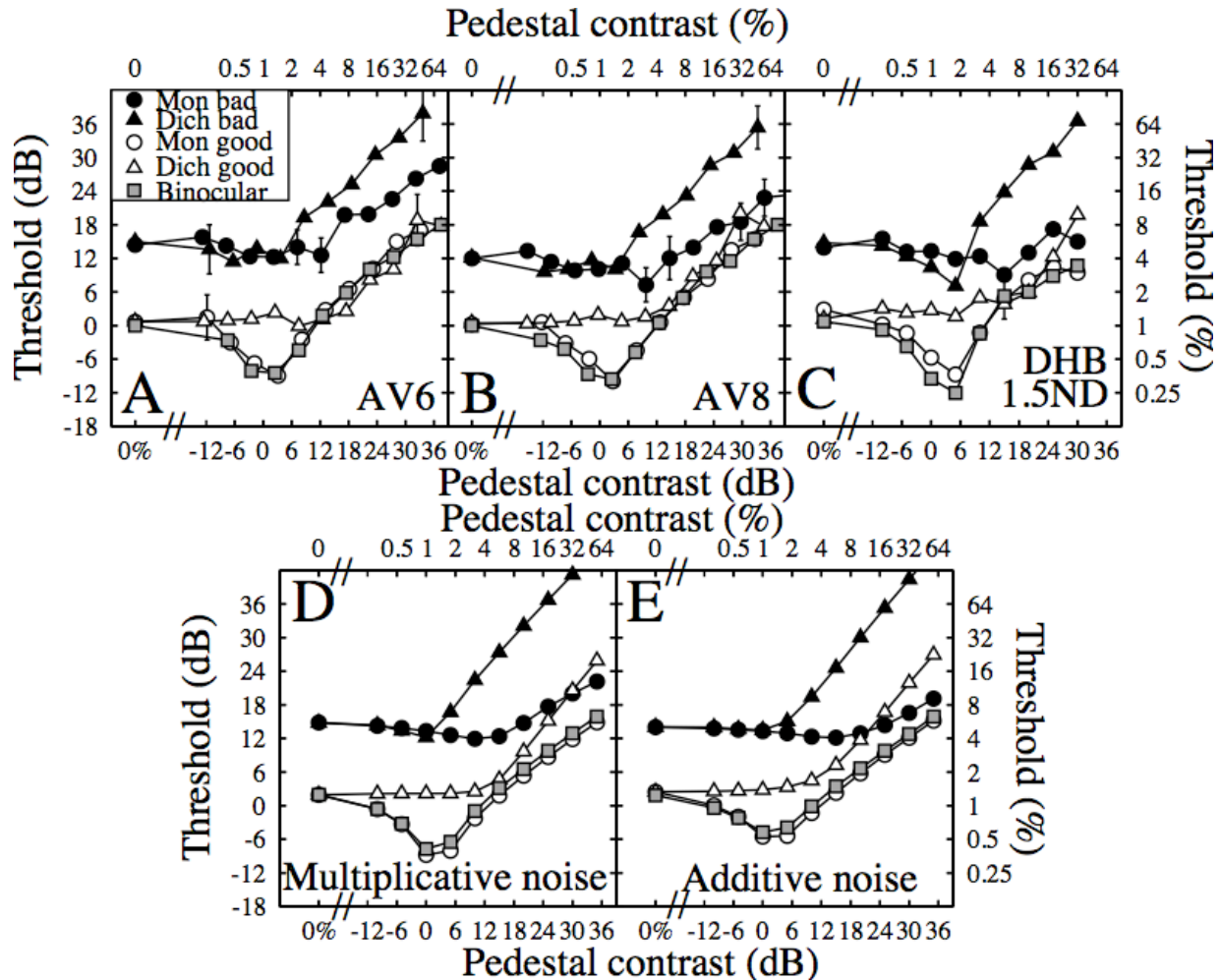
Fig 11: Comparison of AV6, AV8 and DHB (ND) (top row) with two noise models (bottom row). Data are averaged across 6 (A) or eight (B) amblyopes, using the method described in section 2.3.1. Panel C shows data for normal observer DHB with an ND filter in front of one eye (replotted from Figure 2C & F). The model predictions for multiplicative (D; replotted from Fig 10A) and additive (E) noise are the average of 2000 independent simulations, as described in the text.

5.1 Relation with previous contrast masking studies in amblyopia

This is the first study to measure the five logical ocular arrangements of contrast pedestal masking in amblyopic observers. Nevertheless, there are several comparisons to be made with other smaller data sets. Ciuffreda and Fisher (1987) used monocular pedestals and concluded that contrast discrimination is compromised in the bad eye, but they did not measure the entire dipper function. Bradley and Ohzawa (1986) found an amblyopic deficit across the entire dipper function for both of their subjects and similar results were found by Kiper and Kiorpes (1994) in three experimentally strabismic monkeys. In the second two of these studies, monocular facilitation was less in the bad eye than the good eye. The results of Hess *et al.* (1983) and Bradley and Ohzawa (1986) also

showed that that the monocular deficit at high pedestal contrasts is less than that at detection threshold. All of these monocular results are consistent with those for AV6 here.

In the three amblyopes of Levi, Klein & Wang (1994) there was very little difference between the masking functions in the good and bad eyes when plotted on normalized axes, though facilitation (the 'dip') was either absent or shallow in each eye. A recent study by Levi *et al*, (2007) measured monocular contrast discrimination for noise in each eye in ten amblyopic observers (six of whom were strabismic). The noise stimulus was made from a horizontal complex grating with 11 harmonics with random amplitude and phase. Like us, they found that performance was compromised in the amblyopic eye at and above threshold, but unlike us they found that facilitation (the 'dip')

remained intact for the bad eye (as well as the good eye). Levi, Harwerth and Smith (1979, 1980) found that dichoptic facilitation was absent in their two amblyopes (one of whom was strabismic) when testing the bad eye, whereas we found clear evidence that it could remain intact. Whether these different results represent individual differences in amblyopic observers across studies, or differences in stimulus conditions (e.g. horizontal gratings here, vertical gratings in Levi et al, 1979) is not clear.

As reported earlier (section 3.2.3), there is also an inconsistency between the dichoptic results here, and those of Harrad and Hess (1992). In their study, when testing the bad eye of their strabismic amblyopes, masking was stronger than normal and/or stronger than that when testing the good eye. When testing the bad eye here, dichoptic masking was either normal (on threshold normalized axes) or weaker than normal (see Figs 5 and 6). However, just as above, it is unclear whether these different results are due to individual differences amongst amblyopic observers or the use of different stimulus parameters (e.g. orientations were horizontal here, but vertical in Harrad & Hess). Other work also suggests that either or both of these accounts are possible. There is evidence that amblyopic deficits at threshold are greater for vertical than for horizontal contours (Sireteanu and Singer, 1980) and both Agrawal *et al* (2006) and Harrad and Hess (1992) found individual differences in amblyopic dichoptic masking.

Regardless of the reasons for these differences, it is noteworthy that our results bear on the original hypothesis of Harrad and Hess (1992): that amblyopic suppression might be related to normal dichoptic masking. For the amblyopes here, the worst overall performance was for the dichoptic masking condition when testing in the bad eye and, broadly speaking, this deteriorated with an increase in pedestal contrast (solid triangles in Fig 11A & B). We consider this to be an example of amblyopic (strabismic) suppression. Our work with normal observers (Baker & Meese, 2007) shows that dichoptic masking involves both interocular suppression and binocular combination (to produce the 'indirect effect'; see section 4.2.1). And, our modelling here shows that the consequences of these processes are amplified in amblyopia due to the binocular imbalance caused by the attenuator. Of course, our model also includes a component of monocular multiplicative noise, and this also contributes to a loss of sensitivity in the amblyopic eye (we consider this

further in the next subsection).

This also prompts a comparison between the pedestal masking experiments here, and the experiments on binocular rivalry performed by Leonards and Sireteanu (1993). The relation between rivalry and dichoptic masking is not yet clear, but it is plausible that the two phenomena share the same underlying process of suppression (Baker et al, 2007c; van Boxtel, van Ee & Erkelens, 2007). Leonards and Sireteanu (1993) pointed out that the timecourse for binocular rivalry is abnormal in amblyopes, but found that this abnormality could be simulated in normal observers with the use of a neutral density filter in front of one eye. Thus, there is a striking parallel between the rivalry study of Leonards and Sireteanu and the dichoptic masking study here.

5.2 Origins of the abnormalities

The most successful model here attributes the amblyopic loss of contrast signal to (i) an attenuator and (ii) abnormal noise, around an early monocular gain control stage of normal contrast vision. Our model is broadly consistent with several other studies that have concluded that contrast attenuation is not the only factor (Kersten, Hess & Plant, 1988) and that unusually high levels of noise are associated with the amblyopic eye (Kersten, Hess & Plant, 1988; Levi and Klein, 2003; Xu *et al.* 2006; Huang *et al.*, 2007; Levi, Klein and Chen, 2007, 2008). Our results might appear to contrast with those of Pelli et al (2004) who concluded that the equivalent input noise in amblyopic cortex was only slightly worse than normal. However, if the amblyopic noise here were multiplicative (as we have considered) then this might resolve the discrepancy, since Pelli's equivalent input noise is additive (Levi *et al*, 2007).

There are several possible sources for the monocular attenuation including low gain, mis-matched filters (Levi & Klein, 2003) and undersampling (Levi & Klein, 1986). Our results do not help decide between these possibilities, but whatever the cause, our modelling suggests that the deficit is placed before binocular interactions (interocular suppression and binocular summation).

Single-cell recordings suggest that signal-dependent noise is an intrinsic property of visual neurons (Tolhurst, Movshon & Dean, 1983; though see Gur & Snodderly, 2006) and Levi and Klein (2003) suggested that the variance might be

higher in amblyopia; an idea consistent with our results. Levi and Klein also suggest a specific role for noisy templates in amblyopia. Whether this idea is consistent with our model and results depends upon how the template is implemented and the origins of the noise. Some workers (e.g. Nielsen, Watson & Ahumada, 1985) treat the 'template' as the expected response to the signal, distributed across a set of (spatially tuned) sensors (filter-elements). A decision variable is generated by comparing this with the set of actual responses in each stimulus interval. The template matching would be noisy if either the template were corrupted from interval-to-interval (late template noise), or there was variation in the weight of each filter-element contributing to the signal representation (early weighting noise). In this general arrangement, the template is placed late, just before the decision, and therefore after binocular summation in our model. However, this 'late template noise' conflicts with our model, where the amblyopic noise is early, in the amblyopic eye, and before binocular summation and the subsequent decision. On the other hand, this scheme might survive if the amblyopic noise were 'early weighting noise', in which case this might propogate to the binocular stage from the amblyopic eye.

A second interpretation of a 'template' is that it represents a weighting function that is cross-correlated with the signal (e.g. McIlhagga & Paakkonen, 1999). In our model, this can be treated as filter convolution (Dosher & Lu, 1999) in the amblyopic eye before binocular summation. If the template (filter) is systematically mismatched to the signal, then this results in attenuation (as pointed out above), but if the corruption varies from interval-to-interval (McIlhagga & Paakkonen, 1999) then it will produce signal dependent noise. This second interpretation of a noisy template is consistent with our model and results.

Another clue to the possible origins of the amblyopic noise comes from the results of the normal observer with the ND filter. If the filter were serving merely to diminish the effective signal, then this observer's results should be well described by the attenuator model (section 4.2.2). However, the loss of monocular facilitation (Fig 2C) in the filtered eye indicates that the effect of reducing luminance is not simply equivalent to optical attenuation. As for amblyopic observers (e.g. Kersten *et al*, 1988), something else must be involved. One possibility is that low luminance might simply increase the variance of the response

in the filtered eye. However, the results of Bradley and Ohzawa (1986) suggest otherwise. They measured monocular dipper functions for normal observers at low and high luminances. They do not report how monocular viewing was achieved, but presumably by patching the unstimulated eye, thereby presenting it with a negligible level of luminance. When lumiance was reduced in the test eye they found that sensitivity was depressed across the entire dipper function but, notably, the 'dip' region was prevalent and deep. This suggests that the loss of DHB's dip here is due to the influence of the relatively high (and irrelevant) luminance in the other eye, implying a role for variable interocular luminance interactions. Whether this reflects variations in standing levels of interocular suppression (Morrone *et al.*, 1982; Baker *et al.*, 2007c) or luminance combination across the eyes remains unclear. The possibility that mean luminance (the DC component of the stimulus) serves as a mask is not new, and has been refered to as 'zero-frequency masking' (Yang *et al.*, 1995). In particular, Yang and Stevenson (1999) found that the DC component in one eye can mask the detection of low spatial frequency gratings in the other eye. Their results imply only modest masking effects for the 3 c/deg grating (mainly) used here, though if the interaction fluctuates, as we suggest, this is possibly all that is needed. For instance, of the ~12dB of amblyopic sensitivity loss in the model at detection threshold (see Fig 11D), ~9dB is caused by the attenuator and only ~3dB by the multiplicative noise. Clearly, more work is needed to investigate this general idea further.

6 Summary and conclusions

Previous work on contrast discrimination of gratings in normal observers led to a two-stage gain control model of contrast vision. Here we lesioned the model to describe the abnormalities found in amblyopic contrast vision. Our results suggest that the binocular interactions of summation and interocular suppression remain intact in strabismic amblyopia. Several of the amblyopic effects were simulated by attenuating the contrast response in the amblyopic eye, but this was insufficient to account for all of the effects. The model was improved by increasing the noise in the amblyopic eye.

We also found that strabismic amblyopia could be simulated by placing an ND filter in front of one eye of a normal observer. This implies that the reduction of luminance in a normal eye serves both to reduce signal and increase noise.

8 References

Agrawal, R., Conner, I.P., Odom, J.V., Schwartz, T.L. and Mendola, J.D. (2006). Relating binocular and monocular vision in strabismic and anisometropic amblyopia. *Arch Ophthalmol*, 124: 844-850

Asper, L., Crewther, D. and Crewther, S. G. (2000). Strabismic amblyopia, part 1: psychophysics, *Clin Exp Optom,* 83: 49–58.

Baker, D.H. and Meese, T. S. (2007). Binocular contrast interactions: dichoptic masking is not a single process, *Vision Res*, 47: 3096-3107.

Baker, D.H. and Meese, T.S. and Georgeson, M.A. (2007a). Binocular interaction: contrast matching and contrast discrimination are predicted by the same model. *Spatial Vis*, 20: 397-413.

Baker, D. H., Meese, T. S., Mansouri, B. and Hess, R. F. (2007b). Binocular summation of contrast remains intact in strabismic amblyopia, *Invest Ophthalmol Vis Sci*, 48: 5332-5338.

Baker, D.H., Meese, T.S. and Summers, R.J. (2007c). Psychophysical evidence for two routes to suppression before binocular summation of signals in human vision, *Neuroscience*, 146: 435-448.

Barnes G.R., Hess R.F., Dumoulin S.O., Achtman R.L. and Pike G.B. (2001). The cortical deficit in humans with strabismic amblyopia. *J Physiol.*, 533: 281-297

Bex P.J., Mareschal I., and Dakin S.C. (2007). Contrast gain control in natural scenes. *J Vis*. 31;7(11):12.1-12

Blake, R. and Levinson, E. (1977). Spatial properties of binocular neurones in the human visual system, *Exp Brain Res* 27: 221–232.

Bradley, A. and Freeman, R. D. (1981). Contrast sensitivity in anisometropic amblyopia, *Invest Ophthalmol Vis Sci* 21: 467–76.

Bradley, A. and Ohzawa, I. (1986). A comparison of contrast detection and discrimination. *Vision Res*, 26: 991-997.

Burton, G. J. (1981). Contrast discrimination by the human visual system, *Biol Cybern* 40: 27–38.

Campbell F.W. and Green, D.G. (1965). Monocular versus binocular visual acuity, *Nature*, 208: 191-192.

Campbell, F. W. and Kulikowski, J. J. (1966). Orientational selectivity of the human visual system, *J Physiol* 187: 437–45.

Ciuffreda, K. J. and Fisher, S. K. (1987). Impairment of contrast discrimination in amblyopic eyes, *Ophthalmic Physiol Opt* 7: 461–7.

Clatworthy, P.L., Chirimuuta, M., Lauritzen, J.S. and Tolhurst, D.J. (2003). Coding of the contrasts in natural images by populations of neurons in primary visual cortex (V1). *Vision Res*, 43: 1983-2001.

de Belsunce, S. and Sireteanu, R. (1991). The time course of interocular suppression in normal and amblyopic subjects, *Invest Ophthalmol Vis Sci* 32: 2645–52.

De Valois, R.L., Morgan, H. and Snodderly, D.M. (1974). Psychophysical studies of monkey vision. 3. Spatial luminance contrast sensitivity tests of macaque and human observers. *Vision Res*, 14: 75-81.

Ding, J. and Sperling, G. (2006). A gain-control theory of binocular combination. *Proc Natl Acad Sci USA*, 103: 1141-1146.

Dosher, B.A. and Lu, Z.L. (1999). Mechanisms of perceptual learning. *Vision Res*, 39: 3197-3221.

Finney, D. J. (1971). *Probit Analysis*, Cambridge University Press.

Foley, J.M. (1994). Human luminance pattern-vision mechanisms: masking experiments require a new model. *J Opt Soc Am A Opt Image Sci Vis*, 11: 1710-1719.

Gilchrist, J. and McIver, C. (1985). Fechner's paradox in binocular contrast sensitivity, *Vision Res* 25: 609–613.

Green, M. and Blake, R. (1981). Phase effects in monoptic and dichoptic temporal integration: flicker and motion detection, *Vision Res* 21: 365–72.

Gur, M. and Snodderly, D.M. (2006). High response reliability of neurons in primary visual cortex (V1) of alert, trained monkeys. *Cereb Cortex*, 16: 888-895.

Harrad, R.A. and Hess, R.F. (1992). Binocular integration of contrast information in amblyopia, *Vision Res* 32: 2135–50.

Harrad, R.A., Sengpiel, F. and Blakemore, C. (1996). Physiology of suppression in strabismic amblyopia. *Br J Ophthalmol*, 80: 373-377.

Heravian-Shandiz, J., Douthwaite, W. A. and Jenkins, T. C. (1991). Binocular interaction with neutral density filters as measured by the visual evoked response, *Optom Vis Sci* 68: 801–806.

Hess, R. F., Bradley, A. and Piotrowski, L. (1983). Contrast-coding in amblyopia. i. differences in the neural basis of human amblyopia, *Proc R Soc Lond B Biol Sci* 217: 309–30.

Hess, R.F., Campbell, F.W. and Zimmern, R. (1980). Differences in the neural basis of human amblyopias: the effect of mean luminance. *Vision Res*, 20: 295-305.

Hess, R.F., Dakin, S.C., Tewfik, M. and Brown, B. (2001). Contour interaction in amblyopia: scale selection. *Vision Res*, 41: 2885-2296.

Hess, R.F. and Field, D.J. (1994). Is the spatial deficit in strabismic amblyopia due to loss of cells or an uncalibrated disarray of cells? *Vision Res* 34: 3397–406.

Hess, R.F. and Howell, E.R. (1977). The threshold contrast sensitivity function in strabismic amblyopia: evidence for a two type classification, *Vision Res* 17: 1049–55.

Hess, R.F., Pointer, J.S., Simmers, A. and Bex, P. (2003). Border distinctness in amblyopia. *Vision Res*, 43: 2255-2264.

Holopigian, K., Blake, R. and Greenwald, M. J. (1986). Selective losses in binocular vision in anisometropic amblyopes, *Vision Res* 26: 621–30.

Holopigian, K., Blake, R. and Greenwald, M. J. (1988). Clinical suppression and amblyopia, *Invest Ophthalmol Vis Sci* **29**: 444–51.

Hood, A. S. and Morrison, J. D. (2002). The dependence of binocular contrast sensitivities on binocular single vision in normal and amblyopic human subjects, *J Physiol* 540: 607–22.

Huang, C., Tao, L., Zhou, Y. and Lu, Z.-L. (2007). Treated amblyopes remain deficient in spatial vision: A contrast sensitivity and external noise study, *Vision Res,* 47: 22–34.

Kersten, D., Hess, R.F. & Plant, G.T. (1988). Assessing contrast sensitivity behind cloudy media. *Clin Vision Sci*, 2: 143-58.

Kiper, D. C. and Kiorpes, L. (1994). Suprathreshold contrast sensitivity in experimentally strabismic monkeys, *Vision Res* 34: 1575–83.

Kontsevich, L.L. and Tyler, C.W. (1994). Analysis of stereothresholds for stimuli below 2.5 c/deg. *Vision Res*, 34: 2317-2329.

Legge, G.E. (1979). Spatial frequency masking in human vision: binocular interactions, *J Opt Soc Am* 69: 838–847.

Legge, G.E. (1984). Binocular contrast summation– i. detection and discrimination., *Vision Res* 24: 373–383.

Legge, G.E. and Foley, J. M. (1980). Contrast masking in human vision, *J Opt Soc Am* 70: 1458–1471.

Legge, G.E. and Gu, Y.C., (1989). Stereopsis and contrast, *Vision Res*, 29: 989-1004.

Legge, G.E. and Rubin, G.S. (1981). Binocular interactions in suprathreshold contrast perception, *Percept Psychophys*, 30: 49-61.

Lema, S.A. and Blake, R. (1977). Binocular summation in normal and stereoblind humans, *Vision Res* 17: 691–695.

Leonards, U. and Sireteanu, R. (1993). Interocular suppression in normal and amblyopic subjects: the effect of unilateral attenuation with neutral density filters, *Percept Psychophys* 54: 65–74.

Levi, D.M. (2007). Image segregation in strabismic amblyopia. *Vision Res*, 47: 1833-1838.

Levi, M. and Harwerth R.S. (1977) Spatio-temporal interactions in anisometropic and strabismic amblyopia. *Invest Ophthalmol Vis Sci*. 16: 90-95.

Levi, D.M., Harwerth, R.S. and Smith III, E.L. (1979). Humans deprived of normal binocular vision have binocular interactions tuned to size and orientation, *Science* 206: 852–854.

Levi, D.M., Harwerth, R.S. and Smith III, E.L. (1980). Binocular interactions in normal and anomalous binocular vision, *Doc Ophthalmol* 49: 303–24.

Levi, D.M. and Klein, S.A. (1986). Sampling in spatial vision. *Nature*, 320: 360-362.

Levi, D.M. and Klein, S.A. (2002). Classification images for detection and position discrimination in the fovea and parafovea. *J Vis*. 2: 46-65.

Levi, D.M. and Klein, S.A. (2003). Noise provides some new signals about the spatial vision of amblyopes, *J Neurosci* 23: 2522–6.

Levi, D.M., Klein, S.A. and Chen, I. (2007). The response of the amblyopic visual system to noise, *Vision Res*, 47: 2531-2542.

Levi, D. M., Klein, S. A., & Chen, I. (2008). What limits performance in the amblyopic visual system: Seeing signals in noise with an amblyopic brain. *J Vis*, 8(4):1, 1-23.

Levi, D.M., Klein, S.A. and Wang, H. (1994). Discrimination of position and contrast in amblyopic and peripheral vision. *Vision Res,* 34: 3293-3313.

Levi, D.M., Klein, S.A. and Yap, Y.L. (1987). Positional uncertainty in peripheral and amblyopic vision, *Vision Res* 27: 581–97.

Levi, D.M., Li, R.W. and Klein, S.A. (2005). "Phase capture" in amblyopia: the influence function for sampled shape. *Vision Res*, 45: 1793-1805.

Levi, D.M., Yu, C., Kuai, S.G. and Rislove, E. (2007). Global contour processing in amblyopia. *Vision Res*, 47: 512-524.

Li, X., Dumoulin, S.O., Mansouri, B., Hess, R.F. (2007). Cortical deficits in human amblyopia: their regional distribution and their relationship to the contrast detection deficit. *Invest Ophthalmol Vis Sci*., 48:1575-1591.

Maehara, G. and Goryo, K. (2005). Binocular, monocular and dichoptic pattern masking, *Optical Review* 12: 76–82.

McKee, S.P., Levi, D.M. and Movshon, J.A. (2003). The pattern of visual deficits in amblyopia. *J Vis*, 3: 380-405.

McIlhagga, W. and Paakkonen, A. (1999). Noisy templates explain area summation. *Vision Res*, 39: 367-372.

Meese, T.S. (2004). Area summation and masking. *J Vis*, 4: 930-943.

Meese, T.S., Georgeson, M.A. and Baker, D.H. (2006). Binocular contrast vision at and above threshold, *J Vis* 6: 1224–1243.

Meese, T.S. and Hess, R.F. (2004). Low spatial frequencies are suppressively masked across spatial scale, orientation, field position, and eye of origin, *J Vis* 4: 843–859.

Meese, T.S. and Summers, R.J. (2007). Area summation in human vision at and above detection threshold. *Proc Biol Sci*, 274: 2891-2900.

Morrone, M.C., Burr, D.C. and Maffei, L. (1982). Functional implications of cross-orientation inhibition of cortical visual cells. i. neurophysiological evidence, *Proc R Soc Lond B Biol Sci* 216: 335–54.

Nachmias, J. and Sansbury, R. V. (1974). Letter: Grating contrast: discrimination may be better than detection, *Vision Res* 14: 1039–1042.

Nielsen, K.R., Watson, A.B. and Ahumada, A.J. Jr. (1985). Application of a computable model of human spatial vision to phase discrimination. *J Opt Soc Am A.*, 2: 1600-1606.

Nelder, J.A. and Mead, R. (1965). A simplex method for function minimization, *Computer Journal* 7: 308–313.

Pardhan, S. and Gilchrist, J. (1992). Binocular contrast summation and inhibition in amblyopia. the influence of the interocular difference on binocular contrast sensitivity, *Doc Ophthalmol* 82: 239–248.

Parraga, C.A., Troscianko, T. and Tolhurst, D.J. (2005). The effects of amplitude-spectrum statistics on foveal and peripheral discrimination of changes in natural images, and a multi-resolution model. *Vision Res*, 45: 3145-3168.

Pelli, D.G., Levi, D.M. and Chung, S.T. (2004). Using visual noise to characterize amblyopic letter identification. *J Vis*, 4: 904-920.

Popple, A.V. and Levi, D.M. (2000) Amblyopes see true alignment where normal observers see illusory tilt. *Proc Natl Acad Sci USA.*, 97: 11667-11672.

Rohaly, A.M., Ahumada, A.J. Jr. and Watson, A.B. (1997). Object detection in natural backgrounds predicted by discrimination performance and models. *Vision Res*, 37: 3225-3235.

Sengpiel, F. and Blakemore, C. (1996). The neural basis of suppression and amblyopia in strabismus, *Eye* 10: 250–8.

Simmers, A.J., Ledgeway, T. and Hess, R.F. (2005) The influences of visibility and anomalous integration processes on the perception of global spatial form versus motion in human amblyopia. *Vision Res,* 45: 449-460.

Sireteanu, R. and Singer, W. (1980). The "vertical effect" in human squint amblyopia, *Exp Brain Res* 40: 354–7.

Stevenson, S.B. and Cormack, L.K. (2000). A contrast paradox in stereopsis, motion detection, and vernier acuity. *Vision Res*, 40: 2881-2884.

Tolhurst, D.J., Movshon, J.A. and Dean, A.F. (1983). The statistical reliability of signals in single neurons in cat and monkey visual cortex. *Vision Res*, 23: 775-785.

Van Boxtel, J. J. A., van Ee, R. & Erkelens, C. J. (2007). Dichoptic masking and binocular rivalry share common perceptual dynamics. *J Vis*, 7(14):3, 1-11.

van Nes, F.L. and Bouman, M.A. (1967). Spatial modulation transfer in the. human eye. *J. Opt. Soc. Am*. 57: 401-406.

Xu, P., Lu, Z., Qiu, Z and Zhou, Y. (2006). Identify mechanisms of amblyopia in Gabor orientation identification with external noise, *Vision Res,* 46: 3748-3760.

Yang, J. and Stevenson, S. B. (1999). Post-retinal processing of background luminance, *Vision Res* 39: 4045–51.

Yang, J., Qi, X. and Makous, W. (1995). Zero frequency masking and a model of contrast sensitivity, *Vision Res* 35: 1965–78.

Zhang, Y., Pham, B.T. and Eckstein, M.P. (2006). The effect of nonlinear human visual system components on performance of a channelized Hotelling observer in structured backgrounds. *IEEE Trans Med Imaging*, 25: 1348-1362.